PHYSICAL REVIEW B **91**, 235413 (2015)

Full counting statistics and shot noise of cotunneling in quantum dots and single-molecule transistors

Kristen Kaasbjerg[1,*] and Wolfgang Belzig[2]
[1]*Department of Condensed Matter Physics, Weizmann Institute of Science, Rehovot 76100, Israel*
[2]*Fachbereich Physik, Universität Konstanz, D-78457 Konstanz, Germany*
(Received 5 April 2015; published 10 June 2015)

We develop a conceptually simple scheme based on a master-equation approach to evaluate the full-counting statistics (FCS) of elastic and inelastic off-resonant tunneling (cotunneling) in quantum dots (QDs) and molecules. We demonstrate the method by showing that it reproduces known results for the FCS and shot noise in the cotunneling regime. For a QD with an excited state, we obtain an analytic expression for the cumulant generating function (CGF) taking into account elastic and inelastic cotunneling. From the CGF we find that the shot noise above the inelastic threshold in the cotunneling regime is inherently super-Poissonian when external relaxation is weak. Furthermore, a complete picture of the shot noise across the different transport regimes is given. In the case where the excited state is a blocking state, strongly enhanced shot noise is predicted both in the resonant and cotunneling regimes.

DOI: 10.1103/PhysRevB.91.235413 PACS number(s): 72.70.+m, 73.23.Hk, 73.63.−b, 05.40.−a

I. INTRODUCTION

The full counting statistics [1] (FCS) of charge transfer in quantum dots (QDs), nanostructures, and molecules is an important component in the characterization of the microscopic processes governing the transport. As the FCS contains the full information about the low-frequency current fluctuations, it provides access to all higher-order moments of the current fluctuations and hence gives insight not encoded in the average value of the current and the shot noise [2] given by the two first moments.

Experimentally, measurements of the FCS have been realized via real-time detection of single-electron tunneling events [3–5], and the FCS of the charge-transfer mechanisms in various conductors ranging from tunnel junctions and resonant tunneling in Coulomb blockaded QDs to Andreev tunneling at a superconductor–normal-metal interface has been characterized [6–12]. Theoretical schemes to evaluate the FCS in different transport regimes [1,13–15] have successfully explained the experimentally measured FCS as well as the observation of super-Poissonian shot noise in resonant tunneling through QDs [16]. Recent theoretical and experimental work has focused on non-Markovian effects due to coupling to external equilibrium baths [17,18] and quantum coherent effects [19], finite-frequency current statistics [20,21], the effect of the electron-phonon interaction on the FCS in molecular contacts [22–28], interaction effects [29–32], as well as the signature of Majorana bound states in the FCS [33].

Transport in the off-resonant regime where the QD levels are located outside the bias window and separated from the chemical potentials of the leads by an energy δ is dominated by cotunneling processes [34]. In cotunneling processes, an electron or hole tunnels, either elastically or inelastically, through the energetically forbidden charge state and only occupies the QD virtually. Inelastic cotunneling processes turn on at bias voltages exceeding the energy Δ of excited QD states and leave a clear fingerprint in the current-voltage characteristics. Such cotunneling spectroscopy is ideal for probing excited states and their lifetime in QDs [35], molecules [36–39], and graphene QDs [40–42]. Recently, the study of energy dissipation [43,44] and heat transport [45] in the cotunneling regime has gained interest. Experimentally, the shot noise in the cotunneling regime has been demonstrated to be super-Poissonian [46–51], in agreement with theoretical predictions [52]. Other theoretical studies have addressed the shot noise in the presence of cotunneling in specific systems [53–55] and the signature of cotunneling-assisted sequential tunneling [56,57] in the shot noise [58].

The evaluation of the FCS taking into account cotunneling has been addressed theoretically [59–61]. However, the FCS in the cotunneling regime where the interplay between elastic and inelastic cotunneling governs the FCS remains unexplored. Due to the difficulty of measuring single cotunneling events without collapsing the virtual intermediate state of a cotunneling process [62], FCS of cotunneling processes has not been studied experimentally. Recent theoretical proposals for probing the cotunneling time $\tau_{\rm cot} \sim \hbar/\delta$ [63,64] may prove useful in that regard.

In this paper, we develop a conceptually simple scheme based on a Markovian master equation description to evaluate the FCS of cotunneling processes. Compared to rigorous perturbative evaluations of shot noise and FCS to next-to-leading order in the tunnel coupling strength $\Gamma = 2\pi\rho|t|^2$ [53,59,60], the approach outlined here does not account for renormalization and broadening of the electronic levels due to quantum fluctuations which give rise to non-Markovian dynamics [59]. However, for $k_BT, eV \gg \Gamma$ and in the cotunneling regime $\delta \gg \Gamma$, non-Markovian effects are suppressed and can be safely neglected [59]. Our approach applies in these regimes, and we show that it recovers results for the shot noise and FCS in the cotunneling regime of simple models obtained with methods taking into account non-Markovian effects [53,59].

We furthermore demonstrate the method by studying the shot noise across transport regimes in a generic model for a QD system with an excited electronic state. In particular, we

*cosby@fys.ku.dk

address the signature in the shot noise of cotunneling-related transport channels as well as the impact on the shot noise in the case where the excited state is a so-called blocking state.

II. MASTER EQUATION APPROACH TO QUANTUM TRANSPORT

Quantum transport in QDs and molecules involving higher-order tunneling processes between the QD and the leads can be described with a T-matrix based master equation approach [65]. In this approach, the rates for tunneling between the QD states are evaluated using a generalized Fermi's golden rule by expanding the T matrix to a desired order in tunnel-coupling Hamiltonian H_T. To lowest and next-to-leading order, this gives rise to *sequential* and *cotunneling* processes, respectively. Compared to rigorous density-matrix approaches, where a formally exact master equation for the reduced density matrix of the QD can be obtained and systematically expanded in H_T (see, e.g., Refs. [66–68]), the T-matrix approach does not account for quantum effects such as broadening and renormalization of the QD levels. It is therefore only applicable in the regime $k_BT,eV \gg \Gamma$ as well as in the Coulomb blockade regime (cotunneling regime), i.e., $\delta \gg \Gamma$. In these regimes, the discrepancy between the T-matrix approach with proper regularized rates and exact perturbation theory vanishes [69].

In the T-matrix approach, the master equation is restricted to the diagonal elements of the reduced density matrix which are equivalent to the occupation probabilities p_m for the QD states—here labeled by a collective index $m = (N,i)$ for charge and excited state (electronic, vibrational,...). The master equation governing their time evolution is given by

$$\dot{p}_m = -p_m \sum_{m' \neq m} \Gamma_{m,m'} + \sum_{m' \neq m} p_{m'} \Gamma_{m',m}. \tag{1}$$

Together with the normalization condition $\sum_m p_m = 1$, it can be solved for the steady-state occupation probabilities $\dot{p}_m = 0$.

Without the normalization condition, the master equation takes the form of the matrix equation

$$\dot{\mathbf{p}} = \mathbf{M}\mathbf{p}, \tag{2}$$

where the diagonal (off-diagonal) elements of $\mathbf{M}$ (an $M \times M$ matrix where M is the total number of QD states) are given by the first (second) sum in Eq. (1). The master-equation matrix $\mathbf{M}$ is singular with the eigenvector of the zero eigenvalue corresponding to the steady-state solution.

The transition rates $\Gamma_{mm'}$ due to tunneling are obtained from the generalized Fermi golden rule

$$\Gamma_{mm'} = \frac{2\pi}{\hbar} \sum_{i'f'} |\langle f|T|i\rangle|^2 \delta(E_f - E_i). \tag{3}$$

Here, $|i/f\rangle = |m/m'\rangle \otimes |i'/f'\rangle$ are products of QD and lead states, the sum is over possible initial $|i'\rangle$ and final $|f'\rangle$ states of the leads, and $T = H_T + H_T G_0 H_T + \cdots$ is the T matrix with $G_0 = \frac{1}{E_i - H_0}$ denoting the Green function of the decoupled QD and leads described by $H_0 = H_{\rm QD} + \sum_\alpha H_\alpha$, $\alpha = L,R$, $H_\alpha = \sum_{k\sigma} \varepsilon_{\alpha k} c^\dagger_{\alpha k\sigma} c_{\alpha k\sigma}$, and $H_T = \sum_{\alpha k\sigma} t_{\alpha k} c^\dagger_{\alpha k\sigma} d_{\alpha\sigma} + \text{H.c.}$.

The lowest-order *sequential* tunneling processes connect neighboring charge states of the QD system. In this case, the master equation takes the form

$$\dot{p}_{N,i}|_{\rm seq} = -p_{N,i} \sum_{\alpha,j} \left(\Gamma^\alpha_{\substack{N+1,j \\ N,i}} + \Gamma^\alpha_{\substack{N-1,j \\ N,i}} \right) + \sum_{\alpha,j} \left[p_{N+1,j} \Gamma^\alpha_{\substack{N,i \\ N+1,j}} + p_{N-1,j} \Gamma^\alpha_{\substack{N,i \\ N-1,j}} \right]. \tag{4}$$

In next-to-leading order, *cotunneling* processes involve tunneling in and out of two leads and may excite the QD but do not change the charge state. These processes give rise to the following additional terms:

$$\dot{p}_{N,i}|_{\rm cot} = -p_{N,i} \sum_{\alpha\beta,j} \Gamma^{\alpha\beta}_{N,ij} + \sum_{\alpha\beta j} p_{N,j} \Gamma^{\alpha\beta}_{N,ji}. \tag{5}$$

Note that the terms with $i = j$ in the two sums cancel. These terms are associated with *elastic* cotunneling processes which do not change the state and therefore do not appear explicitly in the master equation.

In addition to transport-induced transitions, relaxation mechanisms due to coupling to bosonic degrees of freedom of an equilibrium environment (e.g., phonons) give rise to additional transitions between QD states. The transition rate for these processes is given by

$$\Gamma^{\rm rel}_{mm'} = \frac{\gamma_{mm'}}{\hbar} |n_B(\Delta E_{mm'})|, \tag{6}$$

where $\gamma_{mm'}$ determines the relaxation rate, $\Delta E_{mm'} = E_{m'} - E_m$, and n_B is the Bose-Einstein distribution. In the absence of tunneling-induced transition, this results in a thermalized distribution of the QD states.

From the steady-state solution, the current into terminal α can be obtained by evaluating the net rate of electrons,

$$I_\alpha = e \sum_{N,ij} p_{N,i} \left(\Gamma^\alpha_{\substack{N-1,j \\ N,i}} - \Gamma^\alpha_{\substack{N+1,j \\ N,i}} \right) + e \sum_{\substack{N,ij \\ \beta\neq\alpha}} p_{N,i} \left(\Gamma^{\beta\alpha}_{N,ij} - \Gamma^{\alpha\beta}_{N,ij} \right), \tag{7}$$

where the first (second) term is the sequential (cotunneling) current.

III. FULL COUNTING STATISTICS

The main object of interest in counting statistics of charge transfer in QD systems is the probability distribution $P(n,t)$ for n electrons having passed through the system from the source to the drain contact in the time interval t. In practice, it is more convenient to work with the cumulant generating function (CGF) $\mathcal{S}(\chi,t)$ which is defined by

$$e^{\mathcal{S}(\chi,t)} = \sum_n P(n,t) e^{in\chi}, \tag{8}$$

where χ is a counting field and $\mathcal{S}(0,t) = 0$ in order to fulfill the normalization condition $\sum_n P(n,t) = 1$. From the CGF, the cumulants of the current can be obtained as the derivatives with respect to the counting field χ, i.e., $\langle\langle I^m \rangle\rangle = \frac{\partial^m \mathcal{S}(\chi)}{\partial (i\chi)^m}|_{\chi\to 0}$ for the mth cumulant. The average current and the current

noise are given by the first two cumulants. The probability distribution $P(n,t)$ can be obtained by inverting Eq. (8),

$$P(n,t) = \frac{1}{2\pi}\int_0^{2\pi} d\chi\, e^{-in\chi+\mathcal{S}(\chi,t)}, \tag{9}$$

which follows from the fact that $\mathcal{S}(\chi,t)$ is periodic in χ with a period of 2π.

In order to calculate the CGF and the full counting statistics, it is convenient to work with the n-resolved probabilities, $p_m(n,t)$, for the occupation of the states. As above, n here refers to the number of electrons having traversed the junction, and the distribution for the charge transfer is related to the n-resolved probabilities as $P(n,t) = \sum_m p_m(n,t)$.

At the level of the master-equation treatment outlined in the preceding section, the time evolution of the n-resolved probabilities $p_m(n,t)$ is governed by

$$\dot{\mathbf{p}}(n,t) = \sum_{n'} \mathbf{M}(n-n')\mathbf{p}(n',t), \tag{10}$$

where the matrix elements of $\mathbf{M}$ describe the effect of tunneling and relaxation on the occupations $p_m(n,t)$, and it has been assumed that the dynamics is independent of the absolute value of the counting variable n and only depends on the difference $n-n'$. For sequential and cotunneling processes, the change in the counting variable is restricted to the values $n-n' = 0, \pm 1$, implying that $p_m(n,t)$ is only connected to the neighboring probabilities $p_{m'}(n\pm 1,t)$ and $p_{m'\neq m}(n,t)$.

After Fourier transforming Eq. (10) to χ space, the counting-field dependent master equation takes the form

$$\dot{\mathbf{p}}(\chi,t) = \mathbf{M}(\chi)\mathbf{p}(\chi,t) \tag{11}$$

where

$$\mathbf{p}(\chi,t) = \sum_n \mathbf{p}(n,t)e^{in\chi}, \tag{12}$$

and similarly for $\mathbf{M}$.

In the Markovian approximation, the CGF in the stationary limit $t\to\infty$ can be obtained from the eigenvalue $\Lambda_{\min}(\chi)$ of the counting-field dependent matrix $\mathbf{M}(\chi)$ with the smallest real part [13,17], i.e.,

$$\mathcal{S}(\chi,t) = t\,\Lambda_{\min}(\chi), \tag{13}$$

where t is the measurement time. The evaluation of the FCS thus boils down to constructing the matrix $\mathbf{M}(\chi)$ for the Markovian master equation (11) and calculating the eigenvalue $\Lambda_{\min}(\chi)$ from which the cumulants of the current can be obtained.

The method developed by Bagrets and Nazarov [13] applies to sequential tunneling. In this case, the counting-field dependent master equation (11) can be constructed by replacing the rates in the second line of Eq. (4), which reside in the off diagonal of $\mathbf{M}$, by the counting-field dependent rates [13],

$$\Gamma^{\alpha}_{mm'}(\chi) = \Gamma^{\alpha}_{mm'}e^{\pm i\chi}, \tag{14}$$

where $\pm$ is for processes into/out of the counting lead α.

Below we generalize this approach to cotunneling by demonstrating how to construct the χ-dependent matrix $\mathbf{M}(\chi)$ when cotunneling processes are included. Our approach is valid in the regime where $k_BT, eV \gg \Gamma$ or $\delta \gg \Gamma$. In other words, when the tunneling-induced broadening Γ is smaller than one of the other energy scales.

A. χ-dependent master equation for cotunneling

In order to derive the χ-dependent master equation taking into account cotunneling processes, we start by writing up the master equation for the n-resolved probabilities,

$$\begin{aligned}\dot{p}_m(n,t)|_{\rm cot} = &-p_m(n,t)\sum_{m',\alpha\beta}\Gamma^{\alpha\beta}_{mm'}[1-\delta_{\alpha\beta}\delta_{mm'}]\\ &+\sum_{m',\alpha\beta}\Gamma^{\alpha\beta}_{m'm}[\delta_{\alpha\beta}(1-\delta_{mm'})p_{m'}(n,t)\\ &+\delta_{\alpha L}\delta_{\beta R}p_{m'}(n-1,t)+\delta_{\alpha R}\delta_{\beta L}p_{m'}(n+1,t)],\end{aligned} \tag{15}$$

where the terms with $m=m'$ ($m\neq m'$) correspond to elastic (inelastic) cotunneling processes and we are counting the number of electrons n collected in the left lead.

By differentiating Eq. (12) with respect to time and using the identity,

$$\sum_n e^{i\chi n}p(n\pm 1,t) = e^{\mp i\chi}p(\chi,t), \tag{16}$$

we find

$$\begin{aligned}\dot{p}_m(\chi,t)|_{\rm cot} &= -p_m(\chi,t)\sum_{m',\alpha\beta}\Gamma^{\alpha\beta}_{mm'}[1-\delta_{\alpha\beta}\delta_{mm'}] + \sum_{m',\alpha\beta}\Gamma^{\alpha\beta}_{m'm}[\delta_{\alpha\beta}(1-\delta_{mm'})+\delta_{\alpha L}\delta_{\beta R}e^{i\chi}+\delta_{\alpha R}\delta_{\beta L}e^{-i\chi}]p_{m'}(\chi,t)\\ &= p_m(\chi,t)\sum_{m',\alpha\beta}\Gamma^{\alpha\beta}_{mm'}[\delta_{mm'}(\delta_{\alpha\beta}+\delta_{\alpha L}\delta_{\beta R}e^{i\chi}+\delta_{\alpha R}\delta_{\beta L}e^{-i\chi})-1] + \sum_{m'\neq m,\alpha\beta}\Gamma^{\alpha\beta}_{m'm}[\delta_{\alpha\beta}+\delta_{\alpha L}\delta_{\beta R}e^{i\chi}+\delta_{\alpha R}\delta_{\beta L}e^{-i\chi}]p_{m'}(\chi,t)\\ &= p_m(\chi,t)\sum_{m',\alpha\beta}\left[\delta_{mm'}\Gamma^{\alpha\beta}_{mm}(\chi)-\Gamma^{\alpha\beta}_{mm'}\right] + \sum_{m'\neq m,\alpha\beta}\Gamma^{\alpha\beta}_{m'm}(\chi)p_{m'}(\chi,t),\end{aligned} \tag{17}$$

where the χ-dependent rates are defined by

$$\Gamma^{\alpha\beta}_{mm'}(\chi) = \Gamma^{\alpha\beta}_{mm'}(\delta_{\alpha\beta}+\delta_{\alpha L}\delta_{\beta R}e^{i\chi}+\delta_{\alpha R}\delta_{\beta L}e^{-i\chi}). \tag{18}$$

Here, the Kronecker delta $\delta_{\alpha\beta}$ in the first term ensures that the contribution from elastic cotunneling to the rate in the second term inside the square brackets of Eq. (17) is canceled when $\alpha=\beta$. These terms correspond to elastic cotunneling processes involving only one lead and therefore do not affect the counting statistics for the current.

The χ-dependent master equation in Eq. (17) defines the cotunneling contribution to the matrix elements of $\mathbf{M}(\chi)$ in Eq. (11) and is our main formal result. It demonstrates how cotunneling processes can be included on equal footing with sequential tunneling processes by introducing counting-field dependent cotunneling rates [Eq. (18)] in the master equation. Contrary to the conventional master equation for cotunneling [Eq. (5)], the χ-dependent equation (17) contains contributions from elastic cotunneling processes [first term in the last line of Eq. (17)]. This is due to the fact that, while they do not change the state of QD, they contribute to the transport and hence affect the charge-transfer statistics. We end by noting that the χ-dependent elastic cotunneling rates appear in the diagonal elements of $\mathbf{M}(\chi)$, while the χ-dependent inelastic cotunneling rates appear in the off diagonal.

B. FCS of cotunneling

In the following subsections, we show that our approach recovers known results for the FCS [59] and shot noise [52,53] of cotunneling in simple models.

1. Elastic cotunneling through a single level

We start by considering the simple example of elastic cotunneling through a single off-resonant electronic level with energy ε_0. In this case, the χ-dependent master equation (17) reduces to

$$\dot{p}_0(\chi,t) = p_0(\chi,t)\sum_{\alpha\beta}\left[\Gamma_{00}^{\alpha\beta}(\chi)-\Gamma_{00}^{\alpha\beta}\right] \equiv M(\chi)p_0(\chi,t), \tag{19}$$

where

$$\Gamma_{00}^{\alpha\beta} = \frac{\Gamma_\alpha\Gamma_\beta}{2\pi\hbar}\int d\varepsilon\,\frac{1}{(\varepsilon-\varepsilon_0)^2}f_\alpha(\varepsilon)[1-f_\beta(\varepsilon)] \tag{20}$$

is the rate for elastic cotunneling through the level and $\Gamma_{00}^{\alpha\beta}(\chi)$ is the corresponding χ-dependent rate given in Eq. (18).

The χ-dependent matrix $\mathbf{M}(\chi)$ is here a scalar, and the eigenvalue $\Lambda_{\min}(\chi)$, and hence the CGF, can be read off directly from Eq. (19),

$$\mathcal{S}(\chi) = t_0\left[\Gamma_{00}^{LR}(e^{i\chi}-1)+\Gamma_{00}^{RL}(e^{-i\chi}-1)\right]. \tag{21}$$

This CGF corresponds to bidirectional Poisson statistics and is in agreement with previous work on FCS of elastic cotunneling through a single level [see Eq. (7) of Ref. [59]].

For the current and noise we find

$$I = \frac{e}{t_0}\frac{\partial\mathcal{S}}{\partial(i\chi)}\bigg|_{\chi=0} = \Gamma_{00}^{LR}-\Gamma_{00}^{RL}$$
$$= \frac{\Gamma_\alpha\Gamma_\beta}{2\pi\hbar}\int d\varepsilon\,\frac{1}{(\varepsilon-\varepsilon_0)^2}\left[f_L(\varepsilon)-f_R(\varepsilon)\right], \tag{22}$$

and

$$S = \frac{e^2}{t_0}\frac{\partial^2\mathcal{S}}{\partial(i\chi)^2}\bigg|_{\chi=0} = \Gamma_{00}^{LR}+\Gamma_{00}^{RL}$$
$$= \coth\left(\frac{eV}{2k_BT}\right)\frac{\Gamma_\alpha\Gamma_\beta}{2\pi\hbar}\int d\varepsilon\,\frac{1}{(\varepsilon-\varepsilon_0)^2}\left[f_L(\varepsilon)-f_R(\varepsilon)\right], \tag{23}$$

respectively, where $eV=\mu_L-\mu_R$. At finite temperature, the Fano factor $F=S/e|I|$ is given by $F=\coth(eV/2k_BT)$. In the limit $k_BT\gg eV$, the noise reduces to the equilibrium Johnson-Nyquist noise $S=2G_dk_BT$ where G_d is the conductance. For $eV\gg k_BT$, shot noise becomes dominant with a Poissonian Fano factor $F=1$ as expected for independent tunneling processes.

2. Elastic and inelastic cotunneling through a two-level system

Next, we consider cotunneling trough a system which, in addition to its ground state $|0\rangle$, has an excited electronic state $|1\rangle$ with energy Δ relative to the ground state. In this case, inelastic cotunneling processes induce transitions between the ground and excited states. The steady-state occupation probabilities of the states are given by (see Appendix A)

$$p_0 = \frac{\Gamma_{10}}{\Gamma_{10}+\Gamma_{01}} \quad\text{and}\quad p_1 = \frac{\Gamma_{01}}{\Gamma_{10}+\Gamma_{01}}, \tag{24}$$

where $\Gamma_{ij}=\Gamma_{ij}^{\rm rel}+\sum_{\alpha\beta}\Gamma_{ij}^{\alpha\beta}$ is the total transition rate due to relaxation and inelastic cotunneling.

To obtain the CGF, we set up the counting-field dependent master-equation matrix following Eqs. (17) and (18),

$$\mathbf{M}(\chi) = \begin{pmatrix}\Gamma_{00}(\chi)-\Gamma_{01} & \Gamma_{10}(\chi)\\ \Gamma_{01}(\chi) & \Gamma_{11}(\chi)-\Gamma_{10}\end{pmatrix}, \tag{25}$$

where the counting-field dependent rates are defined as

$$\Gamma_{ii}(\chi) = \Gamma_{ii}^{LR}(e^{i\chi}-1)+\Gamma_{ii}^{RL}(e^{-i\chi}-1) \tag{26}$$

and

$$\Gamma_{ij}(\chi) = \Gamma_{ij}^{\rm rel}+\Gamma_{ij}^{LL}+\Gamma_{ij}^{RR}+e^{i\chi}\Gamma_{ij}^{LR}+e^{-i\chi}\Gamma_{ij}^{RL}, \tag{27}$$

respectively. Note that $\Gamma_{ii}(\chi=0)=0$, implying that the standard master-equation matrix [Eq. (A1)] is recovered for $\chi=0$. The derivatives of the counting-field dependent rates, which will be needed below, are given by

$$\frac{\partial\Gamma(\chi)}{\partial(i\chi)} = \Gamma_{LR}e^{i\chi}-\Gamma_{RL}e^{-i\chi} \tag{28}$$

$$\frac{\partial^2\Gamma(\chi)}{\partial(i\chi)^2} = \Gamma_{LR}e^{i\chi}+\Gamma_{RL}e^{-i\chi}, \tag{29}$$

for both the elastic and inelastic cotunneling rates.

From the relevant eigenvalue of the counting-field dependent master-equation matrix (25), the CGF is found to be

$$\mathcal{S}(\chi) = \frac{t_0}{2}\Big[\Gamma_{00}(\chi)+\Gamma_{11}(\chi)-\Gamma_{10}-\Gamma_{01}$$
$$+\sqrt{[\Gamma_{01}-\Gamma_{10}-\Gamma_{00}(\chi)+\Gamma_{11}(\chi)]^2+4\Gamma_{01}(\chi)\Gamma_{10}(\chi)}\Big]. \tag{30}$$

This CFG is a new result and describes the FCS of combined elastic and inelastic cotunneling. The FCS can be interpreted as arising due to switching between different bidirectional Poisson statistics, as discussed further below.

The current and shot noise can be obtained from the χ derivatives of the CGF. In agreement with the standard master-equation calculation in Appendix A, we find for the current

$$\begin{aligned} I &= \frac{e}{t_0}\frac{\partial \mathcal{S}}{\partial(i\chi)}\bigg|_{\chi=0} \\ &= p_0\partial_{i\chi}\Gamma_{00} + p_1\partial_{i\chi}\Gamma_{11} + p_0\partial_{i\chi}\Gamma_{01} + p_1\partial_{i\chi}\Gamma_{10} \\ &= I_{\rm el} + I_{\rm inel}, \end{aligned} \tag{31}$$

where $I_{\rm el}$ and $I_{\rm inel}$ are elastic and inelastic contributions given by the two first and two last terms in the second line, respectively.

The noise given by the second derivative of the CGF is found to be

$$\begin{aligned} S &= \frac{e^2}{t_0}\frac{\partial^2 \mathcal{S}}{\partial(i\chi)^2}\bigg|_{\chi=0} \\ &= p_0\left(\partial^2_{i\chi}\Gamma_{00} + \partial^2_{i\chi}\Gamma_{01}\right) + p_1\left(\partial^2_{i\chi}\Gamma_{11} + \partial^2_{i\chi}\Gamma_{10}\right) \\ &\quad + \frac{2}{\Gamma_{01}+\Gamma_{10}}[\partial_{i\chi}\Gamma_{01}\partial_{i\chi}\Gamma_{10} - \partial_{i\chi}\Gamma_{00}\partial_{i\chi}\Gamma_{11} \\ &\quad + (\partial_{i\chi}\Gamma_{00} + \partial_{i\chi}\Gamma_{11})I - I^2] \\ &= S_{\rm Poisson} + \Delta S, \end{aligned} \tag{32}$$

where the two terms in the second line describe equilibrium Johnson-Nyquist and Poissonian shot noise, and the term in the square brackets is responsible for a non-Poissonian correction ΔS at bias voltages larger than the inelastic threshold $V > \Delta$. We note that this result for the shot noise is in agreement with Ref. [52] [their Eq. (5.5)].

Due to the factor in front of the square brackets, the non-Poissonian correction ΔS diverges for $\Gamma_{01},\Gamma_{10} \to 0$ if, at the same time, $\Gamma_{00} \neq \Gamma_{11}$. The diverging super-Poissonian noise can be understood as follows. In the limit $\Gamma_{01},\Gamma_{10} \to 0$, i.e., for negligible environmental relaxation and vanishing inelastic cotunneling rates, inelastic cotunneling processes change the state of the system at a rate that is slow compared to the rate of elastic cotunneling processes. As the latter dominate the current, this results in a current that switches between different values when $\Gamma_{00} \neq \Gamma_{11}$. Such telegraphic switching between two transport channels with different conductance naturally produces super-Poissonian shot noise.

3. *Quantum dot with a spin-split level*

The shot noise in a QD with a spin-split level has previously been studied with the real-time diagrammatic method in Ref. [53]. This goes beyond the T-matrix approach adopted here by accounting for the broadening and renormalization of the QD levels. Here, we show that the two methods yield identical results for the noise in the regime $k_BT \gg \Gamma$. For $k_BT \sim \Gamma$, the disagreement between the two methods amounts to a small quantitative difference.

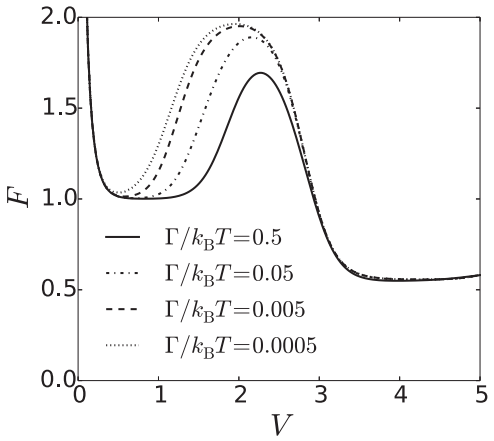

FIG. 1. Fano factor for a QD with a spin-split level for different values of the ratio Γ/k_BT near the cross over between the cotunneling and resonance regimes (see Fig. 3 in Ref. [53] for comparison). Parameters: $\varepsilon_\downarrow = -1.5$, $\varepsilon_\uparrow = 0.5$, $U = 4$, $k_BT = 0.1$, $\Gamma_{L/R} = \Gamma/2$, $\mu_{L/R} = \pm eV/2$.

The Hamiltonian of the QD is given by

$$H_{\rm QD} = \sum_\sigma \varepsilon_\sigma c^\dagger_\sigma c_\sigma + U n_\uparrow n_\downarrow, \tag{33}$$

where ε_σ is the spin-dependent level position and U is the Coulomb interaction for double occupancy of the QD. The sequential and cotunneling rates are calculated as outlined in detail in Sec. IV A below.

In Fig. 1 we show the Fano factor obtained with our approach as a function of bias voltage and for different values of the ratio Γ/k_BT at fixed temperature, $k_BT = 0.1$. With the parameters specified in the caption of Fig. 1, the spin-down level is filled at $V = 0$. The inelastic spin-flip channel opens at $eV = \Delta = \varepsilon_\uparrow - \varepsilon_\downarrow$. At $eV/2 = \varepsilon_\downarrow$ ($eV/2 = \varepsilon_\uparrow + U$), the removal (addition) energy for the spin-down (spin-up) level becomes resonant with the chemical potentials of the drain (source) electrode.

As mentioned above, the agreement with the real-time diagrammatic approach of Ref. [53] is perfect for $k_BT \gg \Gamma$. Remarkably the agreement is even quite good for $k_BT \gtrsim \Gamma$ (for the present parameters less than 10% in the whole bias range for $\Gamma/k_BT = 0.5$). For small values of Γ, the current and noise are dominated by thermally activated sequential tunneling through the two spin levels giving rise to super-Poissonian noise [15]. At larger values of Γ, the change in the Fano factor is due to cotunneling processes. At low bias, elastic cotunneling dominates and results in $F = 1$. Above the inelastic cotunneling threshold at $eV = \Delta$, the state with an electron in the spin-up level becomes populated. After a cotunneling-induced spin flip ($\downarrow \to \uparrow$), the fact that the spin-up level is located inside the bias window, $\varepsilon_\uparrow < eV$, opens for transport through the QD via sequential tunneling. This transport channel remains open until the QD relaxes to the spin-down state via a sequential tunneling or an inelastic cotunneling processes. The transport thus switches between being dominated by elastic cotunneling through the $\downarrow$ level and sequential tunneling through the $\uparrow$ level. As a consequence of

this alternating change in the transport mechanism, the noise becomes super Poissonian.

IV. QUANTUM DOTS AND MOLECULES WITH EXCITED ELECTRONIC STATES

In this section, we consider the shot noise of a QD with an excited electronic state. This could, for example, be a low-energy QD level, a molecular orbital or spin excitations (spin manifolds). We here give a complete picture of the shot noise across the different transport regimes and study, e.g., the signature of the interplay between cotunneling and cotunneling-assisted sequential tunneling (COSET) [56,57] in the shot noise. We furthermore consider the situation where the excited state is a so-called blocking state. This situation is familiar from, e.g., quantum dots and molecules with excited states or broken degeneracies [69–71]. In the resonance regime outside the Coulomb blockaded regions, blocking states give rise to pronounced negative differential conductance (NDC) and strong super-Poissonian noise [72]. In the cotunneling and COSET regimes, the effect of the blocking state on the shot noise has, so far, not been studied, and we find that the noise changes qualitatively in the presence of the blocking state.

A. Generic model and transition rates

We consider a spinless model for a QD where the N electron configuration has an excited electronic state. The states of the QD are described by a set of generic many-body states

$$|N-1\rangle,\ |Na\rangle,\ |Nb\rangle,\ |N+1\rangle, \tag{34}$$

where N refers to the number of electrons on the QD. In a microscopic description of the QD, the states and their energies result from the diagonalization of the underlying microscopic Hamiltonian. The latter are here parametrized as

$$E_{N-1}=0,\quad E_{Na(b)}=\tilde{\varepsilon}_0\,(+\Delta)\quad \text{and}\quad E_{N+1}=2\tilde{\varepsilon}_0+U, \tag{35}$$

where Δ is the energy of the excited N-particle state $|Nb\rangle$ relative to the ground state $|Na\rangle$ with energy $\tilde{\varepsilon}_0=\varepsilon_0-eV_g$ (relative to the $N-1$ state), and U is Coulomb energy associated with the addition of an electron to the N-particle state. With this parametrization, the addition and removal energies of the N-particle ground state become $E_{N+1}-E_{Na}=\tilde{\varepsilon}_0+U$ and $E_{Na}-E_{N-1}=\tilde{\varepsilon}_0$, respectively, implying that the transport gap of the QD is given by U.

To take into account sequential and cotunneling processes, we expand the T matrix to second order in H_T in the calculation of the transition rates. The sequential tunneling rates for adding and removing an electron from the QD are given by

$$\Gamma^{\alpha}_{N-1,Na/b}=\frac{\Gamma_\alpha}{\hbar}\left|M^{\alpha}_{N-1,Na/b}\right|^2 f_\alpha(\varepsilon_{a/b}) \tag{36}$$

$$\Gamma^{\alpha}_{Na/b,N+1}=\frac{\Gamma_\alpha}{\hbar}\left|M^{\alpha}_{Na/b,N+1}\right|^2 f_\alpha(\varepsilon_{a/b}+U) \tag{37}$$

and

$$\Gamma^{\alpha}_{Na/b,N-1}=\frac{\Gamma_\alpha}{\hbar}\left|M^{\alpha}_{N-1,Na/b}\right|^2 [1-f_\alpha(\varepsilon_{a/b})] \tag{38}$$

$$\Gamma^{\alpha}_{N+1,Na/b}=\frac{\Gamma_\alpha}{\hbar}\left|M^{\alpha}_{Na/b,N+1}\right|^2 [1-f_\alpha(\varepsilon_{a/b}+U)], \tag{39}$$

respectively, where $\Gamma_\alpha=2\pi\rho_\alpha|t_\alpha|^2$ is the tunnel broadening, $\varepsilon_{a(b)}=\tilde{\varepsilon}_0\,(+\Delta)$, and the matrix elements between the many-body states are given by

$$M^{\alpha}_{Ni,N-1}=\langle N-1|d_\alpha|Ni\rangle=M^{\alpha*}_{N-1,Ni} \tag{40}$$

$$M^{\alpha}_{Ni,N+1}=\langle N+1|d^\dagger_\alpha|Ni\rangle=M^{\alpha*}_{N+1,Ni}. \tag{41}$$

Here, $d^\dagger_\alpha$,d_α denote the creation and annihilation operators for the single-particle states in the QD system that couple to lead α. For a given microscopic model, the matrix elements can be obtained from the many-body states. Here we treat them as tuneable parameters.

The elastic cotunneling rates for the different states are given by

$$\Gamma^{\alpha\beta}_{N-1}=\frac{\Gamma_\alpha\Gamma_\beta}{2\pi\hbar}\int d\varepsilon\left|\frac{M^{\beta}_{N-1,Na}M^{\alpha}_{Na,N-1}}{\varepsilon-\tilde{\varepsilon}_0}+\frac{M^{\beta}_{N-1,Nb}M^{\alpha}_{Nb,N-1}}{\varepsilon-\tilde{\varepsilon}_0-\Delta}\right|^2 f_\alpha(\varepsilon)[1-f_\beta(\varepsilon)] \tag{42}$$

$$\Gamma^{\alpha\beta}_{N,a}=\frac{\Gamma_\alpha\Gamma_\beta}{2\pi\hbar}\int d\varepsilon\left|\frac{M^{\alpha}_{Na,N-1}M^{\beta}_{N-1,Na}}{\varepsilon-\tilde{\varepsilon}_0}-\frac{M^{\beta}_{Na,N+1}M^{\alpha}_{N+1,Na}}{\varepsilon-\tilde{\varepsilon}_0-U}\right|^2 f_\alpha(\varepsilon)[1-f_\beta(\varepsilon)] \tag{43}$$

$$\Gamma^{\alpha\beta}_{N,b}=\frac{\Gamma_\alpha\Gamma_\beta}{2\pi\hbar}\int d\varepsilon\left|\frac{M^{\alpha}_{Nb,N-1}M^{\beta}_{N-1,Nb}}{\varepsilon-\tilde{\varepsilon}_0-\Delta}-\frac{M^{\beta}_{Nb,N+1}M^{\alpha}_{N+1,Nb}}{\varepsilon-\tilde{\varepsilon}_0-U+\Delta}\right|^2 f_\alpha(\varepsilon)[1-f_\beta(\varepsilon)] \tag{44}$$

$$\Gamma^{\alpha\beta}_{N+1}=\frac{\Gamma_\alpha\Gamma_\beta}{2\pi\hbar}\int d\varepsilon\left|\frac{M^{\alpha}_{N+1,Na}M^{\beta}_{Na,N+1}}{\varepsilon-\tilde{\varepsilon}_0-U}+\frac{M^{\alpha}_{N+1,Nb}M^{\beta}_{Nb,N+1}}{\varepsilon-\tilde{\varepsilon}_0-U+\Delta}\right|^2 f_\alpha(\varepsilon)[1-f_\beta(\varepsilon)]. \tag{45}$$

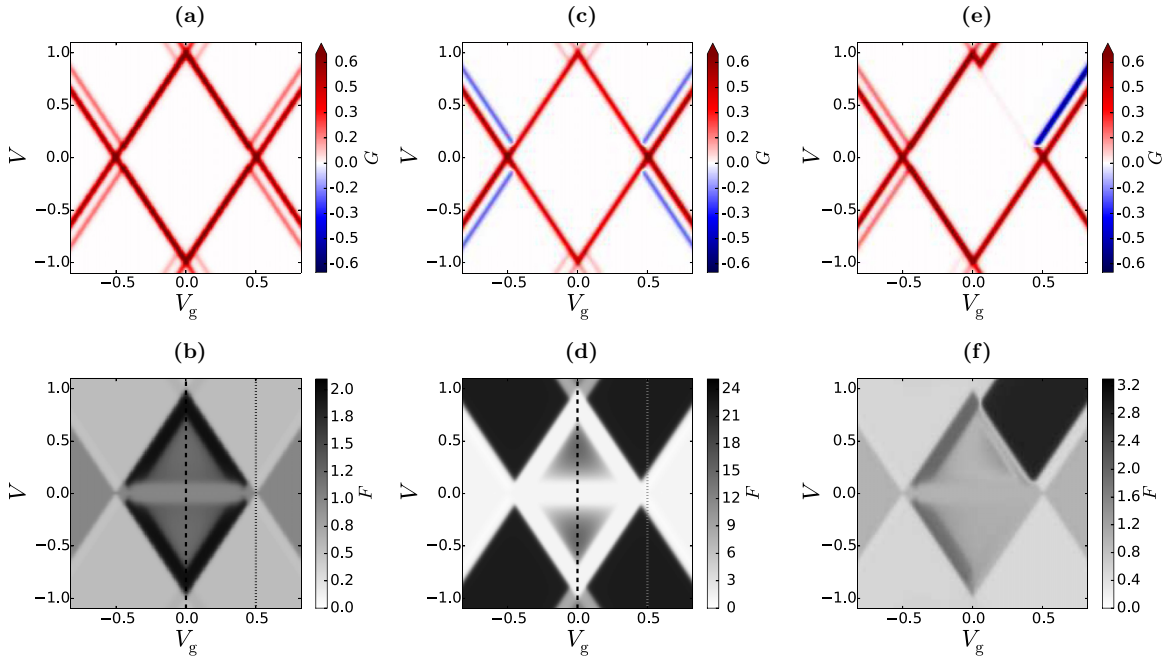

FIG. 2. (Color online) Stability diagrams showing the differential conductance $G = dI/dV$ (upper row) and the Fano factor $F = S/e|I|$ with the thermal contribution to the noise subtracted (lower row) as a function of gate and source-drain voltage for different situations. Note the different color scales in the lower row. (a), (b) The ground and excited N-particle states have identical matrix elements to the $N \pm 1$ states, $M^{L/R}_{Na/b,N\pm1} = 1$. (c), (d) and (e), (f) The excited state is a blocking state with small matrix elements to the $N \pm 1$ states: (c), (d) $M^{L/R}_{N\pm1,Nb} = 0.1$, and (e), (f) $M^{L}_{Nb,N+1} = 0.1$. Matrix elements not specified are equal to unity. Parameters (in units of U): $\varepsilon_0 = -1/2$, $U = 1$, $\Delta = 0.1$, $\Gamma_{L/R} = 0.001$, $k_BT = 0.01$, $\mu_{L/R} = \pm V/2$.

The inelastic cotunneling rates between the ground and excited state of the N-electron configuration are given by

$$\Gamma^{\alpha\beta}_{N,ab} = \frac{\Gamma_a\Gamma_b}{2\pi\hbar}\int d\varepsilon \left| \frac{M^{\alpha}_{Nb,N-1}M^{\beta}_{N-1,Na}}{\varepsilon - \tilde{\varepsilon}_0 - \Delta} - \frac{M^{\beta}_{Nb,N+1}M^{\alpha}_{N+1,Na}}{\varepsilon - \tilde{\varepsilon}_0 - U} \right|^2 f_\alpha(\varepsilon)[1 - f_\beta(\varepsilon - \Delta)] \tag{46}$$

$$\Gamma^{\alpha\beta}_{N,ba} = \frac{\Gamma_a\Gamma_b}{2\pi\hbar}\int d\varepsilon \left| \frac{M^{\alpha}_{Na,N-1}M^{\beta}_{N-1,Nb}}{\varepsilon - \tilde{\varepsilon}_0} - \frac{M^{\alpha}_{Na,N+1}M^{\alpha}_{N+1,Nb}}{\varepsilon - \tilde{\varepsilon}_0 - U + \Delta} \right|^2 f_\alpha(\varepsilon)[1 - f_\beta(\varepsilon + \Delta)]. \tag{47}$$

We evaluate the cotunneling rates at finite temperature and bias with the commonly applied regularization scheme described in Appendix B.

A situation which resembles the conditions for strong super-Poissonian noise discussed below Eq. (32) is realized if the excited state $|Nb\rangle$ is a blocking state which is characterized by having small matrix elements to the other states, i.e., $M^{\alpha}_{Nb,N\pm1} \ll 1$. This leads to strongly reduced cotunneling rates and implies that the inelastic rates and the elastic rate for $|Nb\rangle$ are reduced compared to the elastic cotunneling rate for state $|Na\rangle$. Strong super-Poissonian noise is therefore expected. Since the matrix elements to both the $N \pm 1$ states have to be small in order to suppress the elastic cotunneling rate for $|Nb\rangle$, the shot noise is highly sensitive to the properties of the blocking state via its matrix elements with the neighboring charge states.

B. Stability diagrams and shot noise

We now study the current, conductance, shot noise, and Fano factor for different situations for the blocking property of the excited state $|Nb\rangle$. In the upper row of Fig. 2 we show the differential conductance as a function of gate and source-drain bias voltage—also referred to as charge-stability diagrams—for the cases without [2(a)] and with [2(c) and 2(e)] a blocking state. For the latter, the two plots in Figs. 2(c) and 2(e) correspond to different situations for the matrix elements involving $|Nb\rangle$ (see caption of Fig. 2 for details). Inside the Coulomb blockaded regions where sequential tunneling is suppressed, the current is dominated by cotunneling processes. Due to the linear color scale in the figures, the cotunneling features in the conductance are not visible.

Outside the blockaded regions where sequential tunneling dominate the current, excitation lines going out from the central blockaded region appear at voltages where the excited state enters the bias window. Some of these lines show pronounced NDC when the excited state is a blocking state. Depending on details of the matrix elements for the blocking state, NDC occurs either for both signs [2(c)] or one sign [2(e)] of the gate and bias voltages, and may completely suppress the current [2(e)].

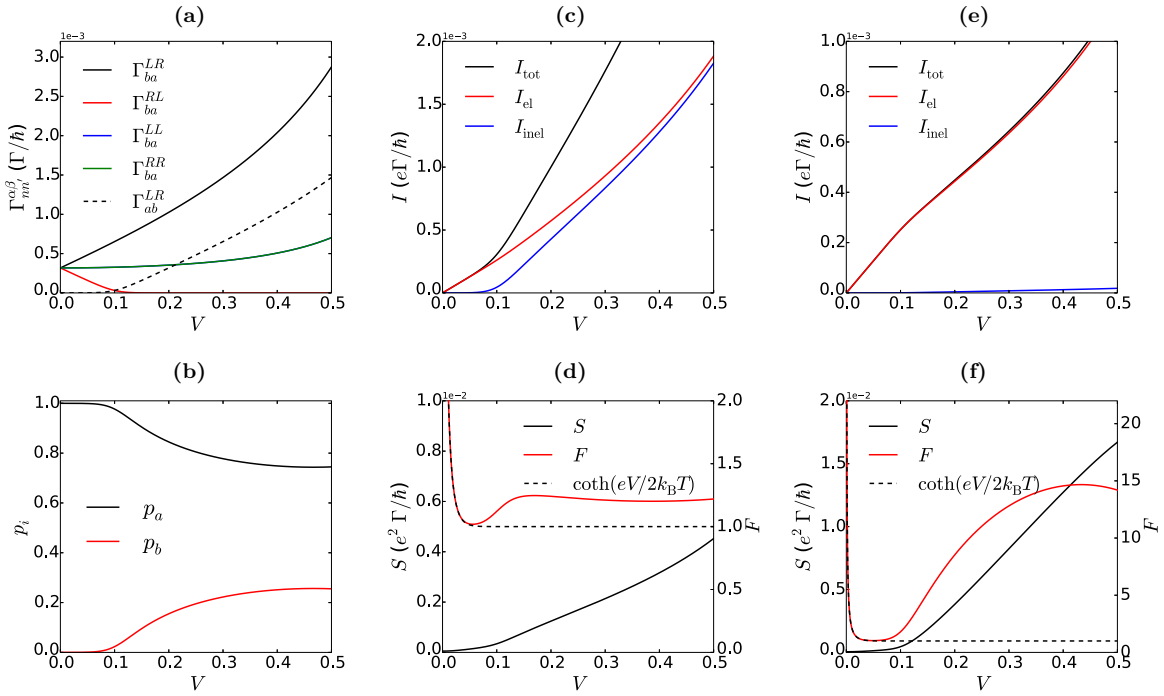

FIG. 3. (Color online) Super-Poissonian noise in the cotunneling regime. (a) Rates for inelastic cotunneling between the $|Na\rangle$, $|Nb\rangle$ states as a function of bias. (b) Occupation probabilities for the $|Na/b\rangle$ states. (c),(d) Cotunneling current [(c)], shot noise [(d) left axis] and Fano factor [(d) right axis] vs bias voltage. (e),(f) Same as in (c),(d) for the situation where the excited state is a blocking state. The plots correspond to the low-bias part of the cuts indicated by dashed lines in Fig. 2(b) [(a)–(d)] and Fig. 2(d) [(e)+(f)].

The corresponding stability diagrams for the Fano factor are shown in the lower row of Fig. 2. Like the conductance, the Fano factors are highly sensitive to the matrix elements of the blocking state. The Fano factors have pronounced features with strong super-Poissonian values in the blockaded regions of the stability diagrams where the signature in the current and conductance is weak. These features originate from the opening of cotunneling related transport channels. In particular, at the threshold for inelastic cotunneling at $V = \Delta$, the Fano factor increases markedly. Also, at the onset of COSET processes near the edges of the blockaded region, the Fano factor shows drastic changes. In the regions outside the blockaded regions where NDC occurs, strong super-Poissonian noise with a large Fano factor is observed. The Fano factor in Fig. 2(f) where the excited state is only partially blocked, shows a mixture of the features present in Figs. 2(b) and 2(d) for no and complete blocking, respectively. In the following subsection, we analyze the shot noise in the different transport regimes in closer detail.

1. Super-Poissonian noise in the cotunneling regime

We start by considering the noise in the cotunneling regime (low-bias part of the cuts through the center of the diamonds in Fig. 2). In this regime, the results based on a pure cotunneling description from Sec. III B 2 apply [Eqs. (31) and (32)].

Figure 3(a)–3(d) summarize the situation without a blocking state corresponding to the stability diagrams in Figs. 2(a) and 2(b). The inelastic cotunneling rates are shown in Fig. 3(a) as a function of bias voltage for the different lead indices. At low temperature, inelastic cotunneling processes in the direction of the voltage drop ($L \to R$) may excite the QD when $V > \Delta$. At the threshold $V = \Delta$, the corresponding rate $\Gamma^{LR}_{N,ab}$ starts to increase linearly with the applied bias. De-excitation processes with rates $\Gamma^{\alpha\beta}_{N,ba}$, which relax the QD back to its ground state, are always possible. The resulting occupation probabilities given in Eq. (24) are shown in Fig. 3(b) with the probability for the ground (excited) state decreasing (increasing) approximately linearly with the bias near the threshold $V \gtrsim \Delta$.

The occupation of the excited state at $V > \Delta$ gives rise to a strong inelastic signal in the current [Fig. 3(c)] corresponding to a positive step in the differential conductance dI/dV. At high bias voltage $V \gg \Delta$, the elastic and inelastic contributions to the total current in Eq. (31) become equal. The shot noise shown in Fig. 3(d) (left axis) together with the Fano factor (right axis), also shows a clear signal at the inelastic threshold. The Fano factor is given by its equilibrium value $F \sim \coth(eV/2k_BT)$ at low bias $V \lesssim k_BT$, drops to the Poissonian value $F = 1$ for $k_BT < V < \Delta$, and becomes super-Poissonian with $F > 1$ for $V > \Delta$. The modest value of the super-Poissonian Fano factor ($F \sim 1.2$) stems from the fact that the elastic and inelastic cotunneling rates are of the same order of magnitude.

Figures 3(e) and 3(f) show the current and shot noise in the case where $|Nb\rangle$ is a blocking state [cut along dashed line in Fig. 2(d)]. In this case, the elastic and inelastic cotunneling rates involving $|Nb\rangle$ are strongly reduced. Therefore, the current in Fig. 3(e) is completely dominated by the elastic component through $|Na\rangle$, and the corresponding differential conductance has a negative step at the inelastic threshold where

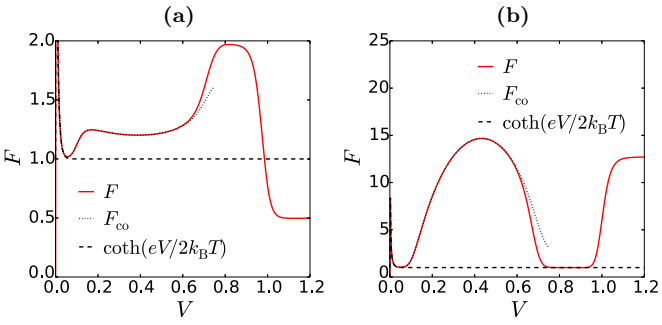

FIG. 4. (Color online) Fano factor in the cotunneling and COSET regime along the cuts marked with dashed lines in the stability diagrams of Fig. 2. The Fano factor F_{co} obtained from the pure cotunneling expressions for the current and noise in Eqs. (31) and (32) is also shown. Above the onset of COSET processes a pure cotunneling description becomes ill defined. The plots correspond to the cuts indicated by dashed lines in Fig. 2(b) [(a)] and Fig. 2(d) [(b)].

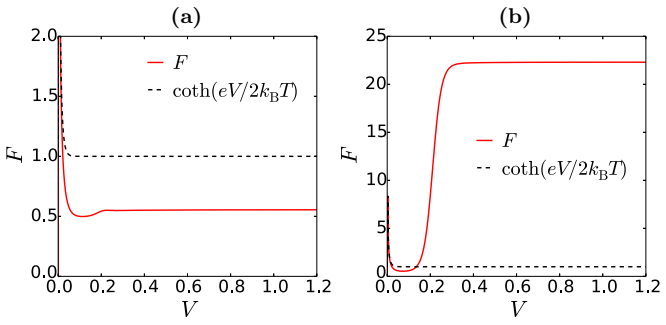

FIG. 5. (Color online) Fano factor in the resonant regime along the cuts marked with dotted lines in the stability diagrams of Fig. 2. The plots correspond to the cuts indicated by dotted lines in Fig. 2(b) [(a)] and Fig. 2(d) [(b)].

the badly conducting excited state becomes populated. The noise in Fig. 3(f), on the other hand, increases nonlinearly with the bias for $V > \Delta$. As a consequence, the Fano factor becomes strongly super-Poissonian with $F \gg 1$. The mechanism behind the increased noise can be understood as telegraphic switching between two elastic current channels with different intrinsic shot noise.

We emphasize that the appearance of strong super-Poissonian noise in the cotunneling regime relies on the excited N-electron state being blocked from both the $N \pm 1$ states, i.e., all the matrix elements $M^{L/R}_{Nb,N\pm1}$ must be small. In addition, the relaxation rate due to coupling to an external equilibrium bath in Eq. (6) must be small compared to the inelastic cotunneling rates, $\Gamma^{\rm rel}_{ab/ba} \ll \Gamma^{\alpha\beta}_{N,ab/ba}$. If this is not the case, the QD relaxes to its ground state on a time scale much faster than the time between cotunneling events. Hence, elastic cotunneling via the ground state will dominate the current and noise and the Fano factor becomes Poissonian $F \sim 1$ in the limit of strong external relaxation.

2. Noise in the COSET regime

To get a clearer picture of the behavior of the noise in the part of the Coulomb blockaded region where cotunneling and sequential tunneling coexist and COSET processes provide a relaxation channel for the excited state, we show in Fig. 4 the bias dependence of the Fano factor along the full cuts (positive bias only) marked with dashed lines in Fig. 2. For comparison, the dotted lines in Fig. 4 show the Fano factor F_{co} obtained from Eqs. (31) and (32) taking into account cotunneling only. At low bias, the noise is dominated by cotunneling processes. As discussed above, the noise becomes super-Poissonian at the threshold for inelastic cotunneling at $V = \Delta$ and acquires a strongly super-Poissonian Fano factor $F \sim 15$ in the presence of the blocking state.

The onset of COSET processes takes place at the side-band resonances at $V = 2|\tilde{\varepsilon}_0 + U - \Delta|$ and $V = 2|\tilde{\varepsilon}_0 + \Delta|$, where relaxation of the excited state $|Nb\rangle$ via sequential tunneling to the $|N \pm 1\rangle$ states becomes possible. In the COSET regime, the change in the Fano factor is qualitative in the two cases. Whereas it increases to a value of $F \sim 2$ without, it drops to $F = 1$ with a blocking state. The increase in the Fano factor in the former case is due to COSET processes where a channel for sequential tunneling inside the blockaded region opens when the excited state becomes populated via inelastic cotunneling [58]. This gives rise to a current that is alternately governed by sequential and cotunneling every time an inelastic cotunneling process excites and de-excites the QD, respectively. However, in the presence of the blocking state, sequential and cotunneling via the excited state are strongly suppressed. The current is therefore dominated by elastic cotunneling via the ground state and the shot noise becomes Poissonian with $F = 1$. This is markedly different from the situation without a blocking state [58]. At bias voltages $V > 2|\tilde{\varepsilon}_0|$ and $V > 2|\tilde{\varepsilon}_0 + U|$, the main resonances enter the bias window and sequential tunneling becomes dominant.

3. Sub-Poissonian noise, NDC, and super-Poissonian telegraphic noise in the resonant regime

Figure 5 shows the bias dependence of the Fano factor along the cuts in the resonant regime outside the Coulomb blockaded regions marked with dashed lines in Fig. 2. In the situation without a blocking state, the Fano factor is sub-Poissonian with $F = 0.5$ for $k_BT < V < 2\Delta$ and a slightly larger value $F \sim 0.55$ for $V > 2\Delta$, which is characteristic for sequential tunneling through a QD with excited states [13,15,73]. However, in the presence of the blocking state, the shot noise becomes strongly super-Poissonian with $F \sim 23$. The mechanism responsible for NDC and the strong enhancement of the noise is the same. When the blocking state enters the bias window, the QD gets trapped in the blocking state due to the small transition rate to other states. This reduces the current and results in a telegraphic noise with long quiet periods without charge transfer interrupted by avalanches of transfer processes every time the QD escapes the blocking state.

V. SUMMARY

In summary, we have demonstrated how the standard scheme to evaluate the FCS of charge transfer due to sequential tunneling in Coulomb blockaded QD systems [13] can be generalized to take into account cotunneling processes.

In analogy with the procedure for sequential tunneling, this is done by replacing the cotunneling rates in the Markovian master equation (1) with counting-field dependent rates as described in Eqs. (17) and (18). This approach neglects non-Markovian effects [53,59,60] associated with tunneling-induced level broadening and shifts, and, hence, only applies for $k_BT, eV \gg \Gamma$ or in the cotunneling regime, $\delta \gg \Gamma$. In the cotunneling regime, we have demonstrated that the results for shot noise and the FCS from more elaborate methods [53,59] are reproduced. In addition, we have obtained an analytic expression for the CGF [Eq. (30)] describing the charge-transfer statistics of elastic and inelastic cotunneling in a two-state QD system.

Studying a generic model for a QD with an excited electronic state, we found that the shot noise in the cotunneling regime is inherently super-Poissonian for voltages larger than the inelastic threshold $V > \Delta$. A strongly enhanced noise level with Fano factor $F \gg 1$ results when the excited state is a so-called blocking state. This is due to telegraphic switching between the two differently conducting channels for elastic cotunneling via the ground and excited state. In the presence of environmental relaxation, the super-Poissonian noise is reduced and becomes Poissonian with $F = 1$ once the relaxation dominates the inelastic cotunneling rates. In the COSET regime where cotunneling and sequential tunneling coexist, we found that the noise is, respectively, super-Poissonian and Poissonian for an excited state without and with blocking properties.

Our approach for evaluating the FCS can be generalized to other higher-order tunneling processes in QD systems, such as, e.g., pair tunneling [74,75] and charge reconfiguration processes in multi-dot systems [76–79], and may be applied to investigate, e.g., the interplay between inelastic cotunneling and quantum interference in the FCS of molecular contacts [80].

ACKNOWLEDGMENTS

We would like to thank A. Nitzan, T. Novotný, and C. Flindt for fruitful discussions. W.B. acknowledges financial support by the DFG through SFB 767, the Kurt Lion Foundation, and an EDEN (Erasmus Mundus Academic Network) grant. K.K. acknowledges support from the Villum and Carlsberg Foundations.

APPENDIX A: MASTER EQUATION FOR ELASTIC AND INELASTIC COTUNNELING IN A TWO-STATE SYSTEM

In this case, the standard master equations takes the form of the 2×2 matrix

$$\mathbf{M} = \begin{pmatrix} -\Gamma_{01} & \Gamma_{10} \\ \Gamma_{01} & -\Gamma_{10} \end{pmatrix}, \tag{A1}$$

where $\Gamma_{ij} = \sum_{\alpha\beta} \Gamma_{ij}^{\alpha\beta}$ are the rates for the inelastic cotunneling-induced transitions between the states. The eigenvalues are found to be

$$\lambda = \tfrac{1}{2}\left[-(\Gamma_{10} + \Gamma_{01}) \pm (\Gamma_{10} + \Gamma_{01})\right], \tag{A2}$$

with the eigenvector of the zero eigenvalue giving the steady-state solution,

$$\mathbf{p}_{\lambda=0} = \left(\frac{\Gamma_{10}}{\Gamma_{01}+\Gamma_{10}}, \frac{\Gamma_{01}}{\Gamma_{01}+\Gamma_{10}}\right)^T. \tag{A3}$$

The current can be obtained from the steady-state solution as

$$\begin{aligned} I &= p_0\left(\Gamma_{00}^{LR} - \Gamma_{00}^{RL}\right) + p_1\left(\Gamma_{11}^{LR} - \Gamma_{11}^{RL}\right) \\ &\quad + p_0\left(\Gamma_{01}^{LR} - \Gamma_{01}^{RL}\right) + p_1\left(\Gamma_{10}^{LR} - \Gamma_{10}^{RL}\right), \\ &= I_{\rm el} + I_{\rm inel}, \end{aligned} \tag{A4}$$

where the first and second line are the elastic $I_{\rm el}$ and inelastic $I_{\rm inel}$ contributions to the current, respectively.

APPENDIX B: REGULARIZED COTUNNELING RATES

The integrals for the elastic and inelastic cotunneling rates can be evaluated using the standard regularization scheme. The procedure for regularizing the diverging integrands in the cotunneling rates of Eqs. (42)–(47) can be found in Ref. [81].

The integrants in the expressions for the cotunneling rates can be written on the general form

$$\begin{aligned} &\left|\frac{A}{\varepsilon - \varepsilon_1 + i0^+} \pm \frac{B}{\varepsilon - \varepsilon_2 + i0^+}\right|^2 \\ &\quad = \left|\frac{A}{\varepsilon - \varepsilon_1 + i0^+}\right|^2 + \left|\frac{B}{\varepsilon - \varepsilon_2 + i0^+}\right|^2 \\ &\qquad \pm 2\mathrm{Re}\left(\frac{A}{\varepsilon - \varepsilon_1 + i0^+}\frac{B}{\varepsilon - \varepsilon_2 - i0^+}\right), \end{aligned} \tag{B1}$$

where we have added a infinitesimal broadening of the QD states (the regularizer) in the denominators.

The regularized rates can then be obtained analytically from the following two integrals,

$$\begin{aligned} \int d\varepsilon\, \frac{f(\varepsilon - E_1)[1 - f(\varepsilon - E_2)]}{(\varepsilon - \varepsilon_1)(\varepsilon - \varepsilon_2)} &= \frac{n_B(E_2 - E_1)}{\varepsilon_1 - \varepsilon_2} \\ \times \mathrm{Re}[\psi(E_{21}^+) - \psi(E_{22}^-) - \psi(E_{11}^+) + \psi(E_{12}^-)] \end{aligned} \tag{B2}$$

and

$$\begin{aligned} &\int d\varepsilon\, \frac{f(\varepsilon - E_1)[1 - f(\varepsilon - E_2)]}{(\varepsilon - \varepsilon_1)^2} \\ &\quad = \frac{n_B(E_2 - E_1)}{2\pi k_B T}\,\mathrm{Im}[\psi'(E_{21}^+) - \psi'(E_{11}^+)], \end{aligned} \tag{B3}$$

where ψ denotes the digamma function, ψ' its derivative, $E_{ij}^{\pm} = \frac{1}{2} \pm \frac{i}{2\pi k_B T}(E_i - \varepsilon_j)$, and n_B the Bose-Einstein distribution.

[1] L. S. Levitov, H. Lee, and G. B. Lesovik, Electron counting statistics and coherent states of electric current, J. Math. Phys. **37**, 4845 (1996).

[2] Y. M. Blanter and M. Büttiker, Shot noise in mesoscopic conductors, Phys. Rep. **336**, 1 (2000).

[3] W. Lu, Z. Ji, L. Pfeiffer, K. W. West, and A. J. Rimberg, Real-time detection of electron tunneling in a quantum dot, Nature (London) **423**, 422 (2003).

[4] C. Fricke, F. Hohls, W. Wegscheider, and R. J. Haug, Bimodal counting statistics in single-electron tunneling through a quantum dot, Phys. Rev. B **76**, 155307 (2007).

[5] S. Gustavsson, R. Leturcq, M. Studer, I. Shorubalko, T. Ihn, K. Ensslin, D. C. Driscoll, and A. C. Gossard, Electron counting in quantum dots, Surf. Sci. Rep. **64**, 191 (2009).

[6] B. Reulet, J. Senzier, and D. E. Prober, Environmental effects in the third moment of voltage fluctuations in a tunnel junction, Phys. Rev. Lett. **91**, 196601 (2003).

[7] Yu. Bomze, G. Gershon, D. Shovkun, L. S. Levitov, and M. Reznikov, Measurement of counting statistics of electron transport in a tunnel junction, Phys. Rev. Lett. **95**, 176601 (2005).

[8] S. Gustavsson, R. Leturcq, B. Simovič, R. Schleser, T. Ihn, P. Studerus, K. Ensslin, D. C. Driscoll, and A. C. Gossard, Counting statistics of single electron transport in a quantum dot, Phys. Rev. Lett. **96**, 076605 (2006).

[9] T. Fujisawa, T. Hayashi, R. Tomita, and Y. Hirayama, Bidirectional counting of single electrons, Science **312**, 1634 (2006).

[10] G. Gershon, Yu. Bomze, E. V. Sukhorukov, and M. Reznikov, Detection of non-gaussian fluctuations in a quantum point contact, Phys. Rev. Lett. **101**, 016803 (2008).

[11] C. Flindt, C. Fricke, F. Hohls, T. Novotný, K. Netočný, T. Brandes, and R. J. Haug, Universal oscillations in counting statistics, Proc. Natl. Acad. Sci. USA **106**, 10116 (2009).

[12] V. F. Maisi, D. Kambly, C. Flindt, and J. P. Pekola, Full counting statistics of andreev tunneling, Phys. Rev. Lett. **112**, 036801 (2014).

[13] D. A. Bagrets and Y. V. Nazarov, Full counting statistics of charge transfer in Coulomb blockade systems, Phys. Rev. B **67**, 085316 (2003).

[14] L. S. Levitov and M. Reznikov, Counting statistics of tunneling current, Phys. Rev. B **70**, 115305 (2004).

[15] W. Belzig, Full counting statistics of super-Poissonian shot noise in multilevel quantum dots, Phys. Rev. B **71**, 161301 (2005).

[16] S. S. Safonov, A. K. Savchenko, D. A. Bagrets, O. N. Jouravlev, Y. V. Nazarov, E. H. Linfield, and D. A. Ritchie, Enhanced shot noise in resonant tunneling via interacting localized states, Phys. Rev. Lett. **91**, 136801 (2003).

[17] C. Flindt, T. Novotný, A. Braggio, M. Sassetti, and A.-P. Jauho, Counting statistics of non-Markovian quantum stochastic processes, Phys. Rev. Lett. **100**, 150601 (2008).

[18] C. Flindt, T. Novotný, A. Braggio, and A.-P. Jauho, Counting statistics of transport through Coulomb blockade nanostructures: High-order cumulants and non-Markovian effects, Phys. Rev. B **82**, 155407 (2010).

[19] H.-B. Xue, H.-J. Jiao, J.-Q. Liang, and W.-M. Liu, Non-markovian full counting statistics in quantum dot molecules, Sci. Rep. **5**, 8978 (2015).

[20] D. Marcos, C. Emary, T. Brandes, and R. Aguado, Finite-frequency counting statistics of electron transport: Markovian theory, New J. Phys. **12**, 123009 (2010).

[21] N. Ubbelohde, C. Fricke, C. Flindt, F. Hohls, and R. J. Haug, Measurement of finite-frequency current statistics in a single-electron transistor, Nat. Commun. **3**, 612 (2012).

[22] J. Koch, M. E. Raikh, and F. von Oppen, Full counting statistics of strongly non-ohmic transport through single molecules, Phys. Rev. Lett. **95**, 056801 (2005).

[23] F. Haupt, T. Novotný, and W. Belzig, Phonon-assisted current noise in molecular junctions, Phys. Rev. Lett. **103**, 136601 (2009).

[24] T. L. Schmidt and A. Komnik, Charge transfer statistics of a molecular quantum dot with a vibrational degree of freedom, Phys. Rev. B **80**, 041307(R) (2009).

[25] R. Avriller and A. Levy Yeyati, Electron-phonon interaction and full counting statistics in molecular junctions, Phys. Rev. B **80**, 041309(R) (2009).

[26] F. Haupt, T. Novotný, and W. Belzig, Current noise in molecular junctions: Effects of the electron-phonon interaction, Phys. Rev. B **82**, 165441 (2010).

[27] D. F. Urban, R. Avriller, and A. Levy Yeyati, Nonlinear effects of phonon fluctuations on transport through nanoscale junctions, Phys. Rev. B **82**, 121414(R) (2010).

[28] Y. Utsumi, O. Entin-Wohlman, A. Ueda, and A. Aharony, Full-counting statistics for molecular junctions: Fluctuation theorem and singularities, Phys. Rev. B **87**, 115407 (2013).

[29] A. O. Gogolin and A. Komnik, Towards full counting statistics for the Anderson impurity model, Phys. Rev. B **73**, 195301 (2006).

[30] D. Urban, J. König, and R. Fazio, Coulomb-interaction effects in full counting statistics of a quantum-dot Aharonov-Bohm interferometer, Phys. Rev. B **78**, 075318 (2008).

[31] G. Schaller, G. Kießlich, and T. Brandes, Transport statistics of interacting double dot systems: Coherent and non-Markovian effects, Phys. Rev. B **80**, 245107 (2009).

[32] D. Kambly, C. Flindt, and M. Büttiker, Factorial cumulants reveal interactions in counting statistics, Phys. Rev. B **83**, 075432 (2011).

[33] D. E. Liu, A. Levchenko, and R. M. Lutchyn, Majorana zero modes choose Euler numbers – revealed by full counting statistics, arXiv:1503.00776.

[34] S. De Franceschi, S. Sasaki, J. M. Elzerman, W. G. van der Wiel, S. Tarucha, and L. P. Kouwenhoven, Electron cotunneling in a semiconductor quantum dot, Phys. Rev. Lett. **86**, 878 (2001).

[35] D. M. Zumbühl, C. M. Marcus, M. P. Hanson, and A. C. Gossard, Cotunneling spectroscopy in few-electron quantum dots, Phys. Rev. Lett. **93**, 256801 (2004).

[36] E. A. Osorio, K. O'Neill, M. Wegewijs, N. Stuhr-Hansen, J. Paaske, T. Bjørnholm, and H. S. J. van der Zant, Electronic excitations of a single molecule contacted in a three-terminal configuration, Nano Lett. **7**, 3336 (2007).

[37] E. A. Osorio, K. Moth-Poulsen, H. S. J. van der Zant, J. Paaske, P. Hedegård, K. Flensberg, J. Bendix, and T. Bjørnholm, Electrical manipulation of spin states in a single electrostatically gated transition-metal complex, Nano Lett. **10**, 105 (2010).

[38] N. Roch, R. Vincent, F. Elste, W. Harneit, W. Wernsdorfer, C. Timm, and F. Balestro, Cotunneling through a magnetic single-moleculetransistor based on N@C_{60}, Phys. Rev. B **83**, 081407(R) (2011).

[39] B. W. Heinrich, L. Braun, J. I. Pascual, and K. J. Franke, Protection of excited spin states by a superconducting energy gap, Nat. Phys. **9**, 765 (2013).

[40] S. Schnez, F. Molitor, C. Stampfer, J. Güttinger, I. Shorubalko, T. Ihn, and K. Ensslin, Observation of excited states in a graphene quantum dot, Appl. Phys. Lett. **94**, 012107 (2009).
[41] X. L. Liu, D. Hug, and L. M. K. Vandersypen, Gate-defined graphene double quantum dot and excited state spectroscopy, Nano Lett. **10**, 1623 (2010).
[42] C. Volk, C. Neumann, S. Kazarski, S. Fringes, S. Engels, F. Haupt, A. Müller, and C. Stampfer, Probing relaxation times in graphene quantum dots, Nat. Commun. **4**, 1753 (2013).
[43] L. Simine and D. Segal, Vibrational cooling, heating, and instability in molecular conducting junctions: Full counting statistics analysis, Phys. Chem. Chem. Phys. **14**, 13820 (2012).
[44] Y. Dinaii, A. Shnirman, and Y. Gefen, Statistics of energy dissipation in a quantum dot operating in the cotunneling regime, Phys. Rev. B **90**, 201404 (2014).
[45] N. M. Gergs, C. B. M. Hörig, M. R. Wegewijs, and D. Schuricht, Charge fluctuations in nonlinear heat transport, Phys. Rev. B **91**, 201107(R) (2015).
[46] E. Onac, F. Balestro, B. Trauzettel, C. F. J. Lodewijk, and L. P. Kouwenhoven, Shot-noise detection in a carbon nanotube quantum dot, Phys. Rev. Lett. **96**, 026803 (2006).
[47] G. Kiesslich, E. Schöll, T. Brandes, F. Hohls, and R. J. Haug, Noise enhancement due to quantum coherence in coupled quantum dots, Phys. Rev. Lett. **99**, 206602 (2007).
[48] Y. Zhang, L. DiCarlo, D. T. McClure, M. Yamamoto, S. Tarucha, C. M. Marcus, M. P. Hanson, and A. C. Gossard, Noise correlations in a Coulomb-blockaded quantum dot, Phys. Rev. Lett. **99**, 036603 (2007).
[49] O. Zarchin, Y. C. Chung, M. Heiblum, D. Rohrlich, and V. Umansky, Electron bunching in transport through quantum dots in a high magnetic field, Phys. Rev. Lett. **98**, 066801 (2007).
[50] N. Ubbelohde, C. Fricke, F. Hohls, and R. J. Haug, Spin-dependent shot noise enhancement in a quantum dot, Phys. Rev. B **88**, 041304 (2013).
[51] Y. Okazaki, S. Sasaki, and K. Muraki, Shot noise spectroscopy on a semiconductor quantum dot in the elastic and inelastic cotunneling regimes, Phys. Rev. B **87**, 041302 (2013).
[52] E. V. Sukhorukov, G. Burkard, and D. Loss, Noise of a quantum dot system in the cotunneling regime, Phys. Rev. B **63**, 125315 (2001).
[53] A. Thielmann, M. H. Hettler, J. König, and G. Schön, Cotunneling current and shot noise in quantum dots, Phys. Rev. Lett. **95**, 146806 (2005).
[54] I. Weymann, J. Barnaś, and S. Krompiewski, Transport through single-wall metallic carbon nanotubes in the cotunneling regime, Phys. Rev. B **78**, 035422 (2008).
[55] A. Carmi and Y. Oreg, Enhanced shot noise in asymmetric interacting two-level systems, Phys. Rev. B **85**, 045325 (2012).
[56] V. N. Golovach and D. Loss, Transport through a double quantum dot in the sequential tunneling and cotunneling regimes, Phys. Rev. B **69**, 245327 (2004).
[57] R. Schleser, T. Ihn, E. Ruh, K. Ensslin, M. Tews, D. Pfannkuche, D. C. Driscoll, and A. C. Gossard, Cotunneling-mediated transport through excited states in the coulomb-blockade regime, Phys. Rev. Lett. **94**, 206805 (2005).
[58] J. Aghassi, M. H. Hettler, and G. Schön, Cotunneling assisted sequential tunneling in multilevel quantum dots, Appl. Phys. Lett. **92**, 202101 (2008).
[59] A. Braggio, J. König, and R. Fazio, Full counting statistics in strongly interacting systems: Non-Markovian effects, Phys. Rev. Lett. **96**, 026805 (2006).
[60] Y. Utsumi, D. S. Golubev, and G. Schön, Full counting statistics for a single-electron transistor: Nonequilibrium effects at intermediate conductance, Phys. Rev. Lett. **96**, 086803 (2006).
[61] C. Emary, Counting statistics of cotunneling electrons, Phys. Rev. B **80**, 235306 (2009).
[62] S. Gustavsson, M. Studer, R. Leturcq, T. Ihn, K. Ensslin, D. C. Driscoll, and A. C. Gossard, Detecting single-electron tunneling involving virtual processes in real time, Phys. Rev. B **78**, 155309 (2008).
[63] A. Romito and Y. Gefen, Weak measurement of cotunneling time, Phys. Rev. B **90**, 085417 (2014).
[64] O. Zilberberg, A. Carmi, and A. Romito, Measuring cotunneling in its wake, Phys. Rev. B **90**, 205413 (2014).
[65] H. Bruus and K. Flensberg, *Many-body Quantum Theory in Condensed Matter Physics* (Oxford University Press, Oxford, 2004).
[66] C. Timm, Tunneling through molecules and quantum dots: Master-equation approaches, Phys. Rev. B **77**, 195416 (2008).
[67] M. Leijnse and M. R. Wegewijs, Kinetic equations for transport through single-molecule transistors, Phys. Rev. B **78**, 235424 (2008).
[68] S. Koller, M. Grifoni, M. Leijnse, and M. R. Wegewijs, Density-operator approaches to transport through interacting quantum dots: Simplifications in fourth-order perturbation theory, Phys. Rev. B **82**, 235307 (2010).
[69] G. Begemann, S. Koller, M. Grifoni, and J. Paaske, Inelastic cotunneling in quantum dots and molecules with weakly broken degeneracies, Phys. Rev. B **82**, 045316 (2010).
[70] M. Leijnse, W. Sun, M. B. Nielsen, P. Hedegård, and K. Flensberg, Interaction-induced negative differential resistance in asymmetric molecular junctions, J. Chem. Phys. **134**, 104107 (2011).
[71] K. Kaasbjerg and K. Flensberg, Image charge effects in single-molecule junctions: Breaking of symmetries and negative-differential resistance in a benzene single-electron transistor, Phys. Rev. B **84**, 115457 (2011).
[72] A. Thielmann, M. H. Hettler, J. König, and G. Schön, Super-Poissonian noise, negative differential conductance, and relaxation effects in transport through molecules, quantum dots, and nanotubes, Phys. Rev. B **71**, 045341 (2005).
[73] A. Thielmann, M. H. Hettler, J. König, and Gerd Schön, Shot noise in tunneling transport through molecules and quantum dots, Phys. Rev. B **68**, 115105 (2003).
[74] J. Koch, M. E. Raikh, and F. von Oppen, Pair tunneling through single molecules, Phys. Rev. Lett. **96**, 056803 (2006).
[75] M. Leijnse, M. R. Wegewijs, and M. H. Hettler, Pair tunneling resonance in the single-electron transport regime, Phys. Rev. Lett. **103**, 156803 (2009).
[76] L. Gaudreau, S. A. Studenikin, A. S. Sachrajda, P. Zawadzki, A. Kam, J. Lapointe, M. Korkusinski, and P. Hawrylak, Stability diagram of a few-electron triple dot, Phys. Rev. Lett. **97**, 036807 (2006).
[77] C.-Y. Hsieh, Y.-P. Shim, M. Korkusinski, and P. Hawrylak, Physics of lateral triple quantum-dot molecules with controlled electron numbers, Rep. Prog. Phys. **75**, 114501 (2012).

[78] M. Seo, H. K. Choi, S.-Y. Lee, N. Kim, Y. Chung, H.-S. Sim, V. Umansky, and D. Mahalu, Charge frustration in a triangular triple quantum dot, Phys. Rev. Lett. **110**, 046803 (2013).

[79] G. Yoo, J. Park, S.-S. B. Lee, and H.-S. Sim, Anisotropic charge kondo effect in a triple quantum dot, Phys. Rev. Lett. **113**, 236601 (2014).

[80] K. G. L. Pedersen, M. Strange, M. Leijnse, P. Hedegård, G. C. Solomon, and J. Paaske, Quantum interference in off-resonant transport through single molecules, Phys. Rev. B **90**, 125413 (2014).

[81] J. Koch, F. von Oppen, and A. V. Andreev, Theory of the Franck-Condon blockade regime, Phys. Rev. B **74**, 205438 (2006).